# How close are the edges of a closed fracture?

L. Sambuelli [1], C. Calzoni [1]
[1] DITAG, Politecnico di Torino, Torino

Abstract

Introduction

In the night between the 11th and the 12th of April 1997 a fire heavily damaged the "Sacra Sindone" Chapel of the Turin cathedral. One of the restoration steps following the accident consists of the substitution of the irreparably damaged marble blocks covering the inner surfaces of the Chapel dome. We show the results of a research aimed to localize joints in the blocks of "Bigio di Frabosa" marble, quarried for the replacements of the damaged blocks. Detection of fractures in rocks is a well known investigation field (Grandjean and Gourry,1996; Myeong-Jong et al., 2004; Tsoflias et al., 2004; Porsani et al., 2006; Ferrero et al., 2007).

We verified the GPR capability to localize joints that would be able to cause the breakup of the block, during the expensive cut and polishing workmanships performed by numerically controlled machines.

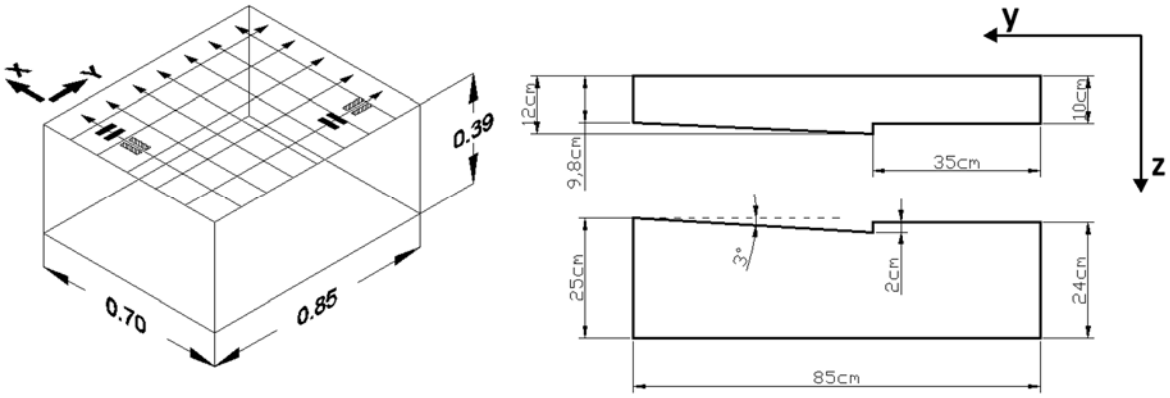


Fig. 1 – Measurements acquisition scheme on the intact block (a), scheme of the block cutting (b).

The first step of the work was the measurements performed on an intact block of "Bigio di Frabosa" marble. We acquired all the GPR measurements with an Aladdin IDS system, which contain in its box two orthogonal 2GHz dipoles: one longitudinal and the other orthogonal to the measure direction; in this way we could appreciate the effect of the polarization direction. We acquired profiles both in the X and Y direction, according to the scheme in Fig 1a. Knowing the dimension of the block we performed a statistical analysis to estimate the velocity of the radar wave (0.097±5×10-4 m/ns) in the block. We processed the data with Reflex Win©, and we verified the absence of internal fractures.

When these preliminary studies were established we created an artificially fracture cutting the block according to the scheme showed in Fig 1b. We performed a cut with two different slopes and a step. We designed the cut at 10 cm below the acquisition plane (roughly corresponding to 2 wavelengths at 2GHz). We investigated the GPR capability to identify different fracture aperture and filling. In detail we performed first a set of acquisitions with the fracture empty. We started disposing the two edges of the joints closed and after with a set of spacers we increased the aperture from 0 to 30mm, in 3 mm steps. Subsequently we filled the fracture with different materials: first with an aluminum foil, after with dry cuttings from stones sawing, successively with a water film and finally with saturated cuttings. For each experiment we adopted an acquisition scheme similar to the one shown in Fig 1. All the experiments

demonstrated that the fracture is easily identifiable by GPR. In Fig 2 the comparison between a radargram acquired on the intact block and one acquired on the cut block with the fracture edges closed without any filling is shown. Even in this case the fracture is visible and the two different slopes and the step can be identified. All the experiments gave similar results both in the single radargrams, and in the 3D models obtained from the data interpolation.

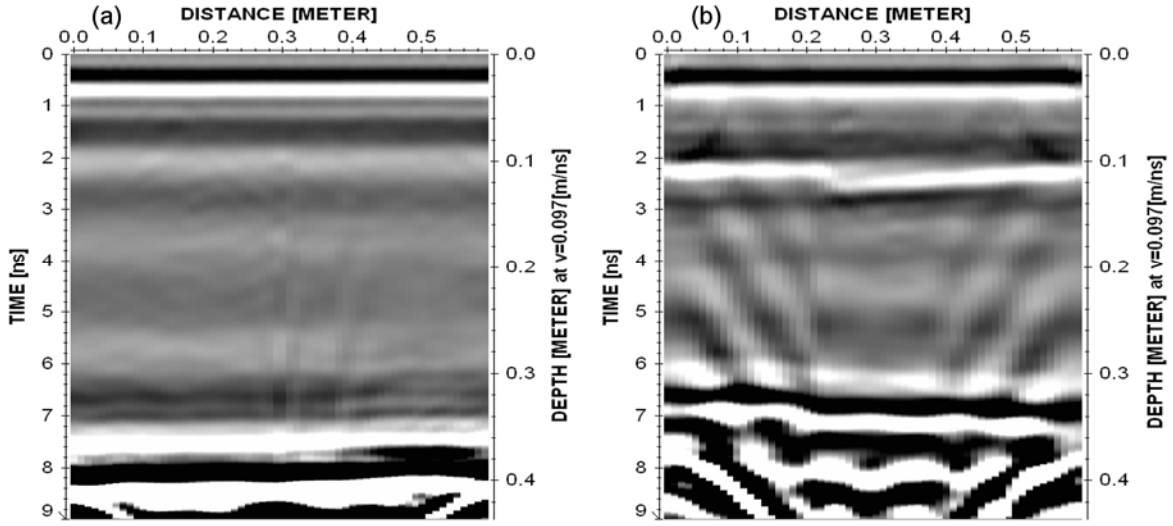


Fig 2 – Radargram corresponding to the measurement on the intact block (a). Radargrams corresponding to the measurements performed on the block after the cut, with the edge of the joint in contact (b).

We then tried to estimate the fracture aperture. Thin layer thickness estimation is an exploited field of research (O'Neill, 2000; Swagata, 2004; Al-Qadi and Lahouar, 2005; Bradford and Deeds, 2006). The analysis of the radar traces in time domain clearly did not show any distinct reflection from the two edges of the fracture. On the other hand it is evident an increasing of the reflection amplitude with the increasing of the fracture aperture. It is also clear the inversion of polarity when the fillings are aluminum or water or saturated cuttings (Fig 3).

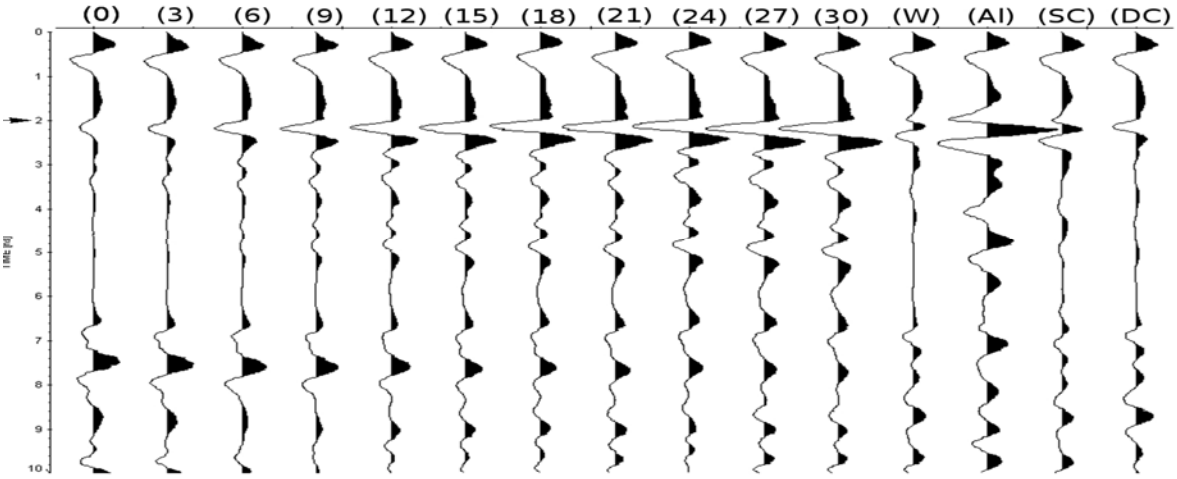


Fig 3 – Comparison among the traces at 10cm (central profile, Y direction, transversal dipoles) obtained with different apertures and fillings. The numbers from 0 to 30 identify the aperture in mm of the joint filled with air. The letters identify the filling materials, respectively: water (W), aluminum (Al), saturated cuttings (SC) and dry cuttings (DC). The arrow on the left indicates the joint position.

Tab 1 – Electromagnetic parameters of the marble and the air.

| | σ [S/m] | εr [-] | F [GHz] | α [1/m] | β [1/m] | λ [m] | V [m/ns] | Z [Ω] |
|---|---|---|---|---|---|---|---|---|
| marble | 7×10-4 | 9.5 | 1.6 | 0.043 | 103.3 | 0.06 | 0.97 | 122.3+i0.05 |
| | | | 2.0 | 0.043 | 129.1 | 0.049 | 0.97 | 122.3+i0.04 |
| air | 1×10-6 | 1 | 1.6 | 1.9×10-4 | 33.5 | 0.19 | 0.3 | 377+i2.1×10-3 |
| | | | 2.0 | 1.9×10-4 | 41.9 | 0.15 | 0.3 | 377+i1.7×10-3 |

We then analyzed the amplitude of the reflected signals. The upper part of the cut block, where the GPR pulse travelled before being reflected by the fracture upper edge, was the same for all the experiments. We could then obtain the reflection coefficient related to each fracture aperture by normalizing the amplitude of reflection obtained from the respective test to the one obtained with the aluminum foil (|R|=1).
We compared the reflection coefficients estimated by the radar measurements with the values estimated with the theoretical formulation, at different air filled fracture aperture. Considering the ratio of the wavelength in air over the fracture aperture, we adopted the thin reflector theory (Annan et al., 1988; Grégoire et al., 2003). We calculated, with the electromagnetic parameters listed in Tab 1, the reflection coefficients at the nominal frequency of the antenna (2GHz) and at the main central frequency of the reflected signals (1.6GHz) as:

$$r=\frac{R\cdot\left(1-e^{iB}\right)}{1-R^{2}\cdot e^{iB}} \quad (1)$$

where:

$$R=\frac{Z_m-Z_a}{Z_m+Z_a} \text{ and } B=4\pi\frac{t_a}{\lambda_a} \quad (2)$$

with Zm and Za respectively the marble and air impedance, ta the aperture of the fracture and λa the wavelength in air. We obtained the values reported in Tab 2.

Tab 2 – Reflection coefficients for the marble-air contrast estimated with the standard formulation (R) and with the thin reflector hypothesis (r) for different apertures ta (2mm, 9mm, 18mm and 27mm) and frequencies (F).

| | F [GHz] | R [-] | r [-] | | | |
|---|---|---|---|---|---|---|
| | | | ta=2mm | ta=9mm | ta=18mm | ta=27mm |
| marble /air | 1.6 | 0.5-i1.5×10-4 | 0.010-i0.09 | 0.18-i0.34 | 0.47-i0.4 | 0.67-i0.31 |
| | 2.0 | 0.5-i1.2×10-4 | 0.016-i0.11 | 0.25-i0.38 | 0.58-i0.36 | 0.75-i0.21 |

In Fig. 4 we plotted, versus each aperture, the mean and the 3 times standard deviation of the experimental values of r estimated by GPR and by the equation (1) at 2GHz. An acceptable fitting is not achieved until the fracture has an aperture of 12mm, which is about 1/12th of the wavelength in air. The best fit is obtained at 1/10th of the wavelength, for higher aperture the fitting worsen even if the theoretical values fall within the experimental ±3 standard deviation range.

Conclusion

According to these experiments the fracture aperture from 1/10th to 1/5th could be estimated by the reflection coefficient analysis. On the other hand we observed that the fitting has been obtained with the upper limit of the frequency band of the reflected signals (2 GHz) and not with its main frequency (1.6 GHz). Moreover in the field activity could not be an easy task to

estimate the actual value of the reflection coefficient, unless setting up a test with a perfect reflector on the opposite side of a representative block.

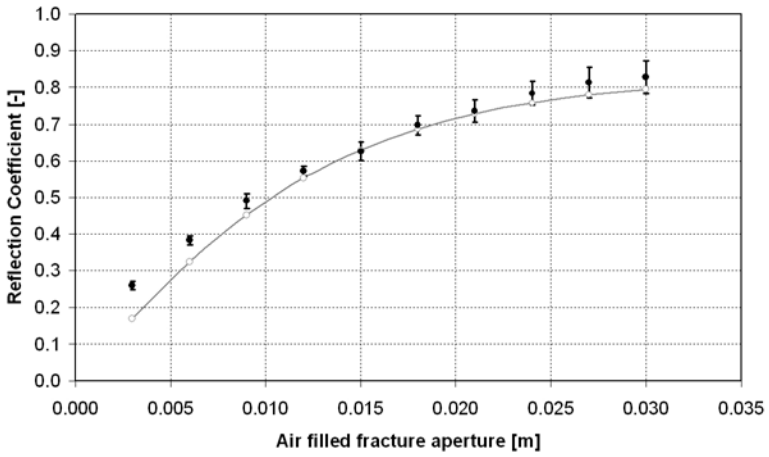


Fig 4 – Comparison between the reflection coefficients estimated from the thin reflector theory (gray line) and the reflection coefficients estimated by radar measurements (black dots) with 3 times the standard deviations (black bar).

**References**

Al-Qadi I.L. and Lahouar S.; 2005: Measuring layer thicknesses with GPR - Theory to practice. Construction and Building Materials, 19(10), 763-772.

Annan, A.P., Davis J.L. and Gendzwill D.; 1988: Radar sounding in potash mines, Saskatchewan, Canada. Geophysics, 53(12), 1556-1564.

Bradford, J.H. and Deeds J.C.; 2006: Ground-penetrating radar theory and application of thin-bed offset-dependent reflectivity. Geophysics, 71(3), K47-K57.

Ferrero, A.M., Godio A., Sambuelli L. and Voyat I.H; 2007: Geophysical and Geomechanical Investigations Applied to the Rock Mass Characterisation for Distinct Element Modelling. Rock Mechanics and Rock Engineering, 40(6), 603-622.

Grandjean, G. and Gourry J.C.; 1996: GPR data processing for 3D fracture mapping in a marble quarry (Thassos, Greece). Journal of Applied Geophysics, 36(1), 19-30.

Grégoire, C., Halleux L. and Vervoort A.; 2003: Application Of Ground Penetrating Radar In A Mining Environment. Mining and Mineral Processing, Sofia.

Myeong-Jong, Y., Jung-Ho K. and Seong-Jun C.; 2004: Integrated application of borehole radar reflection and resistivity tomography to delineate fractures in granite quarry mine. Tenth International Conference on Ground Penetrating Radar, Delft.

O'Neill, K.; 2000: Radar sensing of thin surface layers and near-surface buried objects. Geoscience and Remote Sensing, IEEE Transactions, 38(1), 480-495.

Porsani, J. L., Sauck W.A. and Júnior A.O.S.; 2006: GPR for mapping fractures and as a guide for the extraction of ornamental granite from a quarry: A case study from southern Brazil. Journal of Applied Geophysics, 58(3), 177-187.

Swagata, G.; 2004: Ground Penetrating Radar Response to Thin Layers: Examples from Waites Island, South Carolina. University of South Florida. Masters Thesis.

Tsoflias, G.P., Gestel J.P.V., Stoffa P.L., Blankenship D.D. and Sen M.; 2004: Vertical fracture detection by exploiting the polarization properties of ground-penetrating radar signals. Geophysics, 69(3), 803-810.